Note

Orthometalation reactions in trifluoroacetate dirhodium(II) compounds. Molecular structure of Rh₂(O₂CCF₃)₂[(C₆H₄)PPh₂]₂·(PPh₃)₂·2(C₇H₈)

$Rh_2(O_2CCF_3)_2[(C_6H_4)PPh_2]_2 \cdot (PPh_3)_2 \cdot 2(C_7H_8)$

Francisco Estevan, Pascual Lahuerta*, Eduardo Peris and M. Angeles Ubeda

Departamento de Química Inorgánica, Universitat de Valencia, Dr. Moliner 50, 46100 Burjassot, Valencia (Spain)

Santiago García-Granda, Fermín Gómez-Beltrán and Enrique Pérez-Carreño

Departamento de Química Física y Analítica, Universidad de Oviedo, Julián Clavería s/n, 33006 Oviedo (Spain)

Gabriel González and Manuel Martínez

Departament de Química Inorgánica, Divisió de Ciencies Experimentals i Matemátiques, Universitat de Barcelona, Diagonal 647, 08028 Barcelona (Spain)

Abstract

$Rh_2(O_2CCF_3)_3[(C_6H_4)PPh_2] \cdot (HO_2CCF_3)_2$ reacts with PPh_3 yielding the doubly metalated compound $Rh_2(O_2CCH_3)_2$-$[(C_6H_4)PPh_2]_2 \cdot (HO_2CCF_3)_2$. The reaction proceeds via a reactive intermediate with an equatorial phosphine, Rh_2-$(\eta^2-O_2CCF_3)(\mu-O_2CCF_3)_2[(C_6H_4)PPh_2](PPh_3) \cdot (HO_2CCF_3)$, which can also be generated in moderate yield under photochemical conditions. The structure of the PPh_3 bis-adduct $Rh_2(O_2CCF_3)_2[(C_6H_4)PPh_2]_2 \cdot (PPh_3)_2 \cdot 2(C_7H_8)$ has been determined by X-ray diffraction. $M_r = 1663.27$, orthorhombic, space group $Fdd2$, $a = 41.748(9)$, $b = 21.620(5)$, $c = 17.375(5)$ Å, $V = 15683(6)$ Å³, $Z = 8$, $D_x = 1.41$ g cm⁻³. Mo Kα radiation (graphite crystal monochromator, $\lambda = 0.71073$ Å), μ(Mo Kα) = 5.57 cm⁻¹, $F(000) = 6800$, $T = 293$ K. Final conventional R factor = 0.035 for 2789 'observed' reflections and 422 variables. The molecule shows crystallographic two-fold axis symmetry through the Rh–Rh bond. One toluene solvent molecule slightly disordered is present in the asymmetric unit.

Key words: Crystal structures; Orthometalation; Rhodium complexes; Trifluoroacetate complexes; Dinuclear complexes

---

*Author to whom correspondence should be addressed.

Introduction

In the course of our studies of the reactivity of rhodium(II) compounds with phosphines, we have evidenced that the adduct $Rh_2(O_2CCF_3)_4 \cdot (PPh_3)_2$ (I) in solution, even at room temperature, undergoes stepwise orthometalation of the phosphine ligands [1] much faster than the analogous acetate compound [2] forming the doubly metalated compound $Rh_2(O_2CCF_3)_2$-$[(C_6H_4)PPh_2]_2 \cdot (HO_2CCF_3)_2$ (V). Several intermediates were spectroscopically detected by monitoring the reaction I → V by ³¹P NMR spectroscopy (Scheme 1).

We describe in this paper further studies of the reactivity of $Rh_2(O_2CCF_3)_4$ and $Rh_2(O_2CCF_3)_3$-$[(C_6H_4)PPh_2] \cdot (HO_2CCF_3)_2$ (III) [3] with PPh_3. The crystal structure of the doubly metalated compound V in the form of a bis-phosphine adduct is also reported.

Results and discussion

The reaction of $Rh_2(O_2CCF_3)_4$ with PPh_3 in chloroform or toluene solution has been studied by UV–Vis and ³¹P NMR spectroscopy using different [P]/[Rh₂] ratios in the range 0.2–3.0 and temperatures between −50 and +80 °C. Although the first reaction products detected by ³¹P NMR spectroscopy are axial phosphine adducts of the dirhodium tetratrifluoroacetate, the system slowly evolves at room temperature towards a final mixture of rhodium(II) tetratrifluoroacetate, mono-metalated and doubly metalated compounds, or phosphine adducts of these species. The product distribution obtained even with a [P]/[Rh₂] ratio less than 1 indicates that both the first and the second metalation reactions occur at room temperature.

The ³¹P NMR spectra of samples prepared by mixing triphenylphosphine and rhodium tetratrifluoroacetate in chloroform solution at −40 °C with [P]/[Rh₂] ratios in the range 0.8–2.2 confirm the formation of mono and bis-phosphine adducts in different proportions. The observed final product distribution at room temperature depends on the [P]/[Rh₂] ratio. Even with ratio values lower than 1, substantial amounts of the doubly metalated compound are formed, according to the ³¹P NMR spectrum.

These results show that several equilibria occur in the reaction medium mainly due to the lability of the axial Rh–P bonds in the different dirhodium(II) compounds present in solution. For any [P]/[Rh₂] ratio, even at −40 °C, some rearrangement involving cleavage of the axial Rh–P bond is observed.
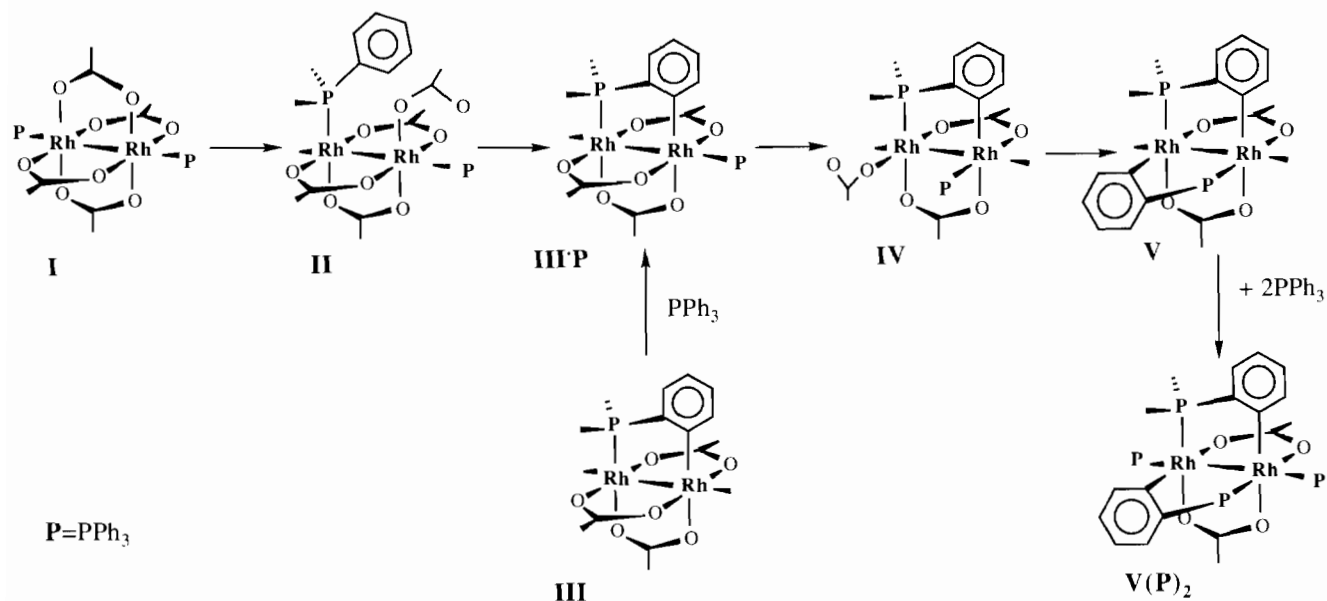
Scheme 1.

Given the high complexity of this reaction system and the fact that $Rh_2(O_2CCF_3)_4$ decomposes in the presence of $[P]/[Rh_2] \gg 2$, we focussed our studies on the more stable and simple reaction system $III + PPh_3$.

The addition of PPh_3 to compound III in $CHCl_3$, $[P]/[Rh_2] = 1$ or 2, allows the spectroscopic detection in solution of the monoadduct $Rh_2(O_2CCF_3)_3[(C_6H_4)PPh_2] \cdot PPh_3$ ($III \cdot PPh_3$) and the bis-adduct $Rh_2(O_2CCF_3)_3[(C_6H_4)PPh_2] \cdot (PPh_3)_2$ ($III \cdot (PPh_3)_2$). These two species only show well resolved spectra at low temperature (-40 °C). At room temperature the broad ^{31}P NMR spectra show that the coordinated phosphine ligands are rapidly exchanging with free phosphine.

The chemical evolution of mixtures of III and PPh_3 in toluene at 60 °C has been monitored by ^{31}P NMR spectroscopy, using $[P]/[Rh_2]$ ratios of 0.5, 1.0 and 1.2. The observed reaction times, 35, 20 and 3 h clearly indicate that phosphine catalysis of the metalation reaction is operating, as already shown in the analogous acetate compounds [2].

Irradiation of an equimolar mixture of III and PPh_3 in $CHCl_3$ at room temperature produces IV in c. 70% yield, with some amounts of V (c. 30%). These solutions allow the direct study of the progress of the $IV \rightarrow V$ reaction step. The completion of this reaction at 45 °C is considerably faster ($t = 1-2$ h) than the overall $III \cdot PPh_3 \rightarrow V$ process in the same conditions (20–30 h). In order to establish a comparison between the relative rates of the two processes ($IV \rightarrow V$ and $III \cdot PPh_3 \rightarrow V$) the evolution of solutions containing mixtures of species $III \cdot PPh_3$, IV and V were studied by ^{31}P NMR spectroscopy. In all cases, while all compound IV has evolved to V no evolution of compound $III \cdot PPh_3$ is detected,

indicating that under these conditions the $III \cdot PPh_3 \rightarrow IV$ step is the rate determining process of the second metalation reaction.

Crystal structure of $V \cdot (PPh_3)_2$

Figure 1 shows a perspective view of the molecule $V \cdot (PPh_3)_2$ with the atomic numbering scheme. Table 1 summarizes the crystal data. Lists of atomic coordinates for the non-hydrogen atoms are given in Table 2. Selected bond distances and angles are given in Table 3.
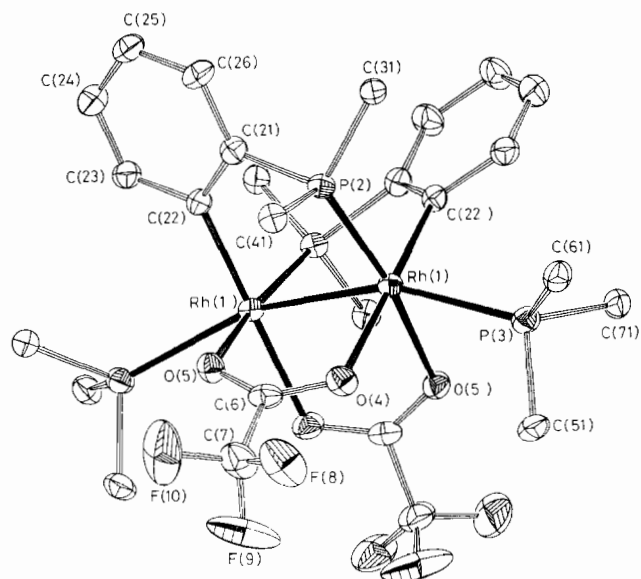
Fig. 1. Perspective view of compound $Rh_2(O_2CCF_3)_2[(C_6H_4)-PPh_2]_2 \cdot (PPh_3)_2$ (V ($PPh_3)_2$) with the atomic numbering. The phenyl rings have been omitted for clarity.

TABLE 1 Crystallographic data for compound $\mathbf{V} \cdot (\mathrm{PPh_3})_2$

Crystal colour	red
Crystal size (mm)	$0.17 \times 0.17 \times 0 17$
Formula	$\mathrm{Rh_2P_4O_4F_6C_{76}H_{58}} \cdot 2(\mathrm{C_7H_8})$
M	1663.27
Space group	$Fdd2$
a (Å)	41.748(9)
b (Å)	21.620(5)
c (Å)	17.375(5)
V (Å^3)	15683(6)
Z	8
λ (Å)	0.71073
D_c (g cm^{-3})	1.41
μ(Mo Kα) (cm^{-1})	5.57
θ Limits	0–25
hkl Range	(0, 0, 0)–(49, 25, 20)
Drift correction	0.99–1.02
Measured reflections	3894
Unique reflections	3555
Observed reflections ($I > 3\sigma(I)$)	2789
$F(000)$	6800
g	0.0008
R^a	0.035
R_{int}	0.020
R_w^b	0.037
No. variables	422
T (K)	293

$^a R = \Sigma(I - \langle I \rangle)/\Sigma I.$ $^b R_w = \Sigma \omega (F_o - F_c)^2$, $\omega = 1/\sigma^2(F_o + gF_o^2)$.

The structure consists of a dinuclear $\mathrm{Rh_2^{4+}}$ unit with two bridging trifluoroacetate ligands and two bridging orthometalated phosphines in a head-to-tail fashion. Both acetate and phosphine ligands are occupying a *cisoid* arrangement. Two molecules of PPh$_3$ occupying the axial sites complete the slightly distorted octahedral coordination around the rhodium atoms.

The Rh(1)–Rh(1′) bond length, 2.630(1) Å, is slightly longer than those found in other related doubly metalated compounds [4]. The angles involving equatorial bonds around each rhodium atom range from 84.0(2) to 94.4(2)°, well within the range of other doubly metalated complexes [4].

The rather long Rh–P bond involving the axial PPh$_3$ molecules, 2.560(2) Å, is indicative of the high *trans* effect of the metal–metal bond. The equatorial Rh–O distances (2.184(5) and 2.187(5) Å) do not show an important difference between the coordination *trans* to carbon and *trans* to phosphorus, as observed for other related metalated compounds with acetate ligands [4].

Experimental

General comments

$\mathrm{Rh_2(O_2CCF_3)_4}$ [5], $\mathrm{Rh_2(O_2CCF_3)_3[(C_6H_4)PPh_2]} \cdot$ $(\mathrm{HO_2CCF_3})_2$ (**III**) [3] and $\mathrm{Rh_2(O_2CCF_3)_2[(C_6H_4)}$-

TABLE 2. Fractional positional and thermal parameters (with e.s.d.s) of $\mathrm{Rh_2(O_2CCH_3)_2[(C_6H_4)PPh_2]} \cdot (\mathrm{PPh_3})_2 \cdot 2(\mathrm{C_7H_8})$ ($\mathbf{V} (\mathrm{PPh_3})_2$)

Atom	x	y	z	U_{eq}^a ($\times 100$)
Rh1	0.00557(1)	0.05985(2)	0.00326(1)	2.84(1)
O4	0.0322(1)	0.0366(3)	0.1074(3)	4.1(2)
O5	−0.0354(1)	0.0652(2)	0.0815(3)	4.1(2)
C6	0.0409(2)	−0.0188(4)	0.1199(5)	4 2(3)
C7	0.0604(3)	−0 0274(5)	0.1921(6)	6.3(4)
F8	0.0785(2)	0 0202(3)	0.2114(4)	9.0(3)
F9	0.0425(2)	−0.0393(5)	0.2522(4)	13.0(4)
F10	0.0802(2)	−0.0753(4)	0 1867(6)	14.6(5)
P2	0.04574(4)	0.0355(1)	−0 0764(1)	3.15(6)
C21	0.0402(2)	−0.0374(4)	−0.1264(5)	3.6(2)
C22	0.0195(2)	−0.0814(4)	−0.0918(4)	3.1(2)
C23	0.0178(2)	−0 1405(4)	−0.1293(5)	3.8(2)
C24	0.0348(2)	−0 1532(4)	−0.1947(6)	5.1(3)
C25	0.0546(2)	−0.1094(4)	−0.2294(5)	5.1(3)
C26	0.0575(2)	−0.0516(4)	−0.1939(5)	5 0(3)
C31	0.0572(2)	0 0872(4)	−0 1566(5)	3.8(2)
C32	0.0849(2)	0.1225(4)	−0 1555(5)	4.7(3)
C33	0 0926(2)	0.1606(5)	−0.2186(7)	6.5(4)
C34	0 0728(3)	0.1616(5)	−0.2829(7)	7 1(4)
C35	0.0453(3)	0.1257(5)	−0.2848(6)	6 3(4)
C36	0.0375(2)	0.0877(4)	−0.2220(5)	5 0(3)
C41	0.0837(2)	0.0227(4)	−0.0259(5)	3 7(2)
C42	0.0950(2)	0.0686(5)	0.0237(5)	5.4(3)
C43	0 1244(2)	0.0623(6)	0.0626(6)	7.2(4)
C44	0 1414(2)	0.0078(6)	0 0540(7)	7.8(5)
C45	0.1296(2)	−0.0392(5)	0.0070(8)	7.6(4)
C46	0.1008(2)	−0.0317(5)	−0.0310(6)	6.0(3)
P3	0.00910(5)	0.1703(1)	0.0558(1)	3.70(6)
C51	−0.0246(2)	0.2212(4)	0.0290(5)	4.2(3)
C52	−0.0218(2)	0.2844(4)	0.0230(5)	5.3(3)
C53	−0.0485(3)	0 3213(4)	0 0042(7)	7.0(4)
C54	−0.0779(3)	0.2946(5)	−0.0060(7)	7.1(4)
C55	−0.0817(2)	0.2314(5)	0.0004(7)	6.8(4)
C56	−0.0553(2)	0 1938(4)	0.0176(6)	5.6(3)
C61	0.0063(2)	0.1719(4)	0.1617(5)	4.4(3)
C62	−0.0202(3)	0.1967(5)	0.1992(6)	5 9(4)
C63	−0.0219(4)	0.1969(7)	0.2778(6)	8.6(5)
C64	0.0027(3)	0.1736(6)	0 3210(6)	8.2(5)
C65	0.0291(3)	0.1476(6)	0.2856(6)	7.1(4)
C66	0 0309(3)	0.1458(5)	0.2051(6)	5 9(4)
C71	0 0443(2)	0.2207(4)	0.0383(5)	4.4(3)
C72	0.0552(2)	0.2252(5)	−0.0360(6)	5.7(4)
C73	0.0819(3)	0.2630(5)	−0.0534(7)	7.0(4)
C74	0.0973(2)	0.2936(5)	0.0021(8)	7.4(4)
C75	0.0862(3)	0.2889(7)	0.0793(8)	9 8(6)
C76	0.0597(3)	0.2539(5)	0 0963(6)	7.1(4)
C81	0.1780(3)	0.2251(5)	0.6905(7)^b	
C82	0.1531(3)	0.2649(5)	0 6673(7)^b	
C83	0.1372(3)	0 3004(5)	0.7213(7)^b	
C84	0.1466(3)	0.2997(5)	0.7985(7)^b	
C85	0.1720(3)	0.2615(5)	0.8212(7)^b	
C86	0.1877(3)	0.2244(5)	0.7674(7)^b	
C87	0.2181(3)	0.1886(5)	0.7908(7)^b	

$^a U_{eq} = \frac{1}{3}\Sigma_i U_{ii}$. ^{b}Common isotropic thermal parameter U_{iso} ($\times 100$) $= 16.2(3)$ Å^2.

TABLE 3. Selected bond distances (Å) and angles (°) and their e.s.d.s for $Rh_2(O_2CCH_3)_2[(C_6H_4)PPh_2] \cdot (PPh_3)_2 \cdot 2(C_7H_8)$ ($V \cdot (PPh_3)_2$)

Rh(1)–O(4)	2.184(5)	Rh(1)–O(5)	2.187(5)	Rh(1)–P(2)	2 237(2)
Rh(1)–P(3)	2.560(2)	Rh(1)–Rh(1')	2 630(1)	Rh(1)–C(22')	2.011(7)
O(5')–Rh(1)–O(4)	84.0(2)	P(2)–Rh(1)–O(4)	94.4(2)	P(2)–Rh(1)–O(5')	169.4(2)
P(3)–Rh(1)–O(4)	83.7(2)	P(3)–Rh(1)–O(5)	77.0(1)	P(3)–Rh(1)–P(2)	113.4(1)
O(4)–Rh(1)–O(22')	179.2(2)	O(5)–Rh(1)–C(22')	96.3(2)	P(2)–Rh(1)–C(22')	86.4(2)
P(3)–Rh(1)–C(22')	96.1(2)	O(5')–Rh(1)–Rh(1')	85.1(1)	O(4)–Rh(1)–Rh(1')	82.1(1)
P(2)–Rh(1)–Rh(1')	84.3(1)	P(3)–Rh(1)–Rh(1')	158.1(1)	C(22')–Rh(1)–Rh(1')	97.7(1)

$PPh_2]_2 \cdot (HO_2CCF_3)_2$ (V) [1] were prepared according to literature procedures.

Preparation of $Rh_2(\eta^2-O_2CCF_3)(\mu-O_2CCF_3)_2[(C_6H_4)$-$PPh_2][PPh_3] \cdot (HO_2CCF_3)_2$ (IV)

III (30 mg, 0.027 mmol) and PPh_3 (7.2 mg, 0.028 mmol) were dissolved with 0.6 ml of $CDCl_3$ inside an NMR tube yielding a brown–red solution. The NMR tube was set in the surface of a photochemical reactor with an Hg-vapour lamp (OSRAM-125). After 40 min of radiation a ^{31}P NMR spectrum was recorded showing the presence of two products: IV (c. 80%) and V (20%). $^{31}P\{^1H\}$ NMR (CH_2Cl_2) spectrum of IV: $\delta(P_a) = 16.2$ ppm, $^1J(Rh-P_a) = 134.0$ Hz, $^2J(Rh-P_a) = 10.3$ Hz, $\delta(P_b) = 40.5$ ppm, $^1J(Rh-P_b) = 192.2$ Hz.

Evolution of the reaction IV → V

Compound IV was prepared *in situ* by the method described above. The NMR tube was introduced in the NMR probe which was previously equilibrated at 45 °C. The reaction was followed by monitoring the disappearance of compound IV and the formation of V ($\delta P = 16.6$ ppm, $^1J(Rh-P) = 162.0$ Hz). Compound V was completely formed after 120 min of reaction.

The same reaction was performed by adding PPh_3 ($[P]/[Rh_2] = 2$) to a freshly prepared solution of IV. No significant differences in the reaction rate were found. The final solution afforded the isolation of the phosphine bis-adduct $Rh_2(O_2CCF_3)_2[(C_6H_4)PPh_2]_2 \cdot (PPh_3)_2$ ($V \cdot (PPh_3)_2$), which was characterized by spectroscopy and X-ray methods. $^{31}P\{^1H\}$ NMR (CH_2Cl_2) spectrum of $V \cdot (PPh_3)_2$, $T = 298$ K: $\delta(P_a) = 14.99$ ppm, $^1J(Rh1-P_a) = 173.0$ Hz, $\delta(P_b) = -5.4$ ppm; $T = 233$ K: $\delta(P_a) = 14.8$ ppm, $^1J(Rh1-P_a) = 170$ Hz, $\delta(P_b) = -4.2$ ppm.

Evolution of the reaction III → V

III (30 mg, 0.027 mmol) and PPh_3 (7.2 mg, 0.028 mmol) were dissolved with 0.6 ml of $CDCl_3$ inside an NMR tube yielding a brown–red solution containing the monoadduct compound $Rh_2(O_2CCF_3)_3[(C_6H_4)$-$PPh_2] \cdot PPh_3$ (III·PPh_3). The tube was introduced in the NMR probe and the temperature was equilibrated at 45 °C. The reaction was followed by monitoring the formation of compound V and the disappearance of

III·PPh_3. Compound V was completely formed after 25 h. The same reaction was repeated using $[P]/[Rh_2]$ ratios of 0.5, 1 and 1.2 at 60 °C. $^{31}P\{^1H\}$ NMR (CH_2Cl_2) spectrum of III·PPh_3 (233 K): $\delta(P_a) = 22.6$ ppm, $^1J(Rh1-P_a) = 149.0$ Hz, $^3J(P_b-P_a) = 6.8$ Hz, $\delta(P_b) = -5.8$ ppm, $^1J(Rh2-P_b) = 113.5$ Hz, $^2J(Rh1-P_b) = 18.5$ Hz.

X-ray crystallographic procedures

Crystallographic constants and experimental details for the structure of compound $V \cdot (PPh_3)_2$ are collected in Table 1. See also 'Supplementary material'.

Experimental data were collected on an Enraf-Nonius CAD4 (ω–2θ scan technique with a maximum scan time of 60 s) using a Mo Kα radiation and a graphite crystal monochromator. Intensity was checked by three standards measured every 60 min. Lorentz and polarisation corrections were applied and a profile analysis was performed on all reflections [6, 7]. The R_{int} results from the averaging of some doubly measured reflections. Empirical absorption corrections were applied [8]. The structure was solved by Patterson methods using DIR-DIF [9] and anisotropically refined using a local version of SHELX76 [10]. One toluene solvent molecule was located and isotropically refined with a fixed idealised geometry. The positions of most hydrogen atoms were refined from their geometrically calculated positions as riding atoms with a common isotropic thermal parameter. Geometrical calculations were done using PARST [11]. The drawing in Fig. 1 was made with EUCLID [12]. Atomic scattering factors were taken from the International Tables for X-ray Crystallography [13].

All calculations were made on a Micro Vax 3400 computer at the Scientific Computer Center of the University of Oviedo.

Supplementary material

Lists of structure amplitudes, anisotropic thermal parameters, H atom parameters, distances, angles, least-squares-planes data and principal torsion angles are deposited in the Cambridge Crystallographic Data Center.

Acknowledgement

References

1 P. Lahuerta, M.A. Ubeda, J. Payá, S. García-Granda, F. Gómez-Beltrán and A. Anillo, *Inorg. Chim. Acta, 205* (1993) 91.

2 P. Lahuerta, J. Payá, M.A. Pellinghelli and A. Tiripicchio, *Inorg. Chem., 31* (1992) 1224, and refs. therein.

3 P. Lahuerta, J. Latorre, E. Peris, M. Sanaú, M.A. Ubeda and S. García-Granda, *J. Organomet. Chem., 445* (1993) C10.

4 (a) E.C. Morrison and D.A. Tocher, *J. Organomet Chem., 408* (1991) 105; (b) *Inorg. Chim. Acta, 157* (1989) 139; (c) A.R. Chakravarty, F.A. Cotton and D.A. Tocher, *J Chem. Soc., Chem. Commun,* (1984) 501; (d) A.R. Chakravarty, F.A. Cotton, D.A. Tocher and J.H. Tocher, *Organometallics,* 4 (1985) 8; (e) P. Lahuerta, R. Martínez-Máñez, J. Payá, E. Peris and W. Díaz, *Inorg. Chim. Acta, 173* (1990) 99.

5 S.A. Johnson, H.R. Hunt and H.M. Neumann, *Inorg Chem., 2* (1963) 960.

6 M.S. Lehman and F.A. Larsen, *Acta Crystallogr., Sect. A, 30* (1974) 580.

7 D.F. Grant and E.J. Gabe, *J Appl. Crystallogr., 11* (1978) 114.

8 N. Walker and D. Stuart, *Acta Crystallogr., Sect. A, 39* (1983) 158.

9 P.T. Beurskens, G. Admiraal, G. Beurskens, W.P. Bosman, S. García-Granda, R.O. Gould, J.M.M. Smits and C. Smykalla, The DIRDIF program system, *Tech Rep.,* Crystallography Laboratory, University of Nijmegen, Netherlands, 1992.

10 (a) G.M. Sheldrick, *SHELX76,* program for crystal structure determination, University of Cambridge, UK, 1976; (b) J.F. Van der Maelen, *Ph.D. Thesis,* University de Oviedo, Spain, 1991.

11 M. Nardelli, *Comput. Chem., 7* (1983) 95.

12 A.L. Spek, in D. Sayre (ed.), *Computational Crystallography,* Clarendon, Oxford, 1982, p. 528.

13 *International Tables for X-ray Crystallography,* Vol. IV, Kynoch, Birmingham, UK, 1974 (present distributor Kluwer, Dordrecht, Netherlands).